DOE/BC/15119-3

(OSTI ID: 807567)

QUANTITATIVE METHODS FOR RESERVOIR CHARACTERIZATION AND IMPROVED RECOVERY: APPLICATION TO HEAVY OIL SANDS

ANNUAL REPORT

October 1, 1999 – September 30, 2000

James W. Castle[1], Principal Investigator
Fred J. Molz[2], Lead Co-Investigator
Robert A. Bridges[1], Cynthia L. Dinwiddie[2], Caitlin J. Lorinovich[1], Silong Lu[2]

October 24, 2000

DE-AC26-98BC15119

Submitted by:
Clemson University
300 Brackett Hall
Box 345702
Clemson, South Carolina 29634

[1]Department of Geological Sciences, Clemson University
[2]Department of Environmental Engineering and Science, Clemson University

Disclaimer

This report was prepared as an account of work sponsored by an agency of the United States Government. Neither the United States Government nor any agency thereof, nor any of their employees, makes any warranty, express or implied, or assumes any legal liability or responsibility for the accuracy, completeness, or usefulness of any information, apparatus, product, or process disclosed, or represents that its use would not infringe privately owned rights. Reference herein to any specific commercial product, process, or service by trade name, trademark, manufacturer, or otherwise does not necessarily constitute or imply its endorsement, recommendation, or favoring by the United States government or any agency thereof. The views and opinions of authors expressed herein do not necessarily state or reflect those of the United States Government or any agency thereof.

Abstract

Comparison and integration of data from field investigations in southern Utah with results from Coalinga Field in California is yielding a better understanding of the distributions of subsurface geological characteristics and petrophysical properties. A new minipermeameter probe was developed for measurement of *in situ* permeability in small-diameter holes drilled in outcrop. Advantages of this method include measurement of permeability below the weathered zone of outcrop surfaces and a superior sealing mechanism around the air injection zone. Field use of the new drill-hole minipermeameter probe has provided data needed for fractal analysis and confirms that that the new technology is a robust and viable field method.

Facies-dependent variations in outcrop permeability values and scale have been identified. Geological and petrophysical contrasts between bioturbated sandstone facies and cross-bedded sandstone facies have important implications for subsurface fluid-flow prediction using outcrop analogs. Fractal scaling properties of the outcrop permeability data collected from southern Utah have been analyzed for application to predicting permeability distributions. Results from geological investigation, permeability testing, and fractal analysis are being integrated to produce conditioned, three-dimensional computer models for reservoir characterization of Coalinga Field.

Table of Contents

Introduction

This project involves application of advanced analytical property-distribution methods conditioned to continuous outcrop control for improved reservoir characterization and simulation. The investigation is being performed in collaboration with Chevron Production Company U.S.A. as an industrial partner, and incorporates data from the Temblor Formation in Chevron's West Coalinga Field, California. Improved prediction of interwell reservoir heterogeneity is needed to increase productivity and to reduce recovery cost for California's heavy oil sands, which contain approximately 2.3 billion barrels of remaining reserves in the Temblor Formation and in other formations of the San Joaquin Valley.

The first part of the project focused on collecting outcrop and subsurface data for characterization and modeling. Data were collected by geological investigation of outcrops near Coalinga, study of cores from Coalinga Field, and geological examination and permeability testing of outcrops in southern Utah (Figures 1 and 2). Petrophysical data from Coalinga Field and outcrop permeability data from southern Utah have been analyzed for fractal structure present in the data sets. The current work involves loading data and building property models in preparation for flow simulation of Coalinga Field.

Results and Discussion

Geological Characterization

To characterize reservoir geometries and trends, depositional and sequence-stratigraphic interpretations of the Miocene Temblor Formation have been made from detailed sedimentological study of outcrops and cores. Approximately 2300 feet of section have been described and interpreted from twelve outcrop localities in the Coalinga area. In addition to the outcrop descriptions, approximately 4470 feet of cores from 13 wells in West Coalinga Field have been studied in detail by Clemson University personnel. These cores are from locations throughout the field and are considered to be representative of the depositional environments and reservoir characteristics.

Two major transgressive-regressive cycles are recognized in the Temblor Formation. A thick lower interval of sand represents deposition on an erosional surface that was incised during lowstand of relative sea level. Incised valleys were filled during subsequent relative sea-level rise, which produced a succession of stacked fining-upward sequences. Marine influence in the valley-fill succession, which reaches a thickness of approximately 45 m, increases upward through estuarine deposits and into marine clay (Figure 3). Regressive deposits of a tide- and wave-dominated shoreline overlie this transgressive systems tract. The regressive accumulation, which becomes coarser grained upward, includes tidal-channel and intertidal-flat deposits. Sand beds containing abundant shell debris separate depositional cycles and serve as useful marker horizons within this interval. The regressive tide- and wave-dominated shoreline deposits are capped by a diatomite, up to 9 m thick, that represents deposition during relative sea-level rise. In the upper part of the Temblor Formation, a regressive tidal and coastal-plain succession of sand and clay overlies the diatomite.

Sediments of the Temblor Formation were deposited on the margin of a forearc basin associated with Miocene initiation of transform motion along an active continental margin. Consequently, Temblor depositional patterns represent the combined effects of sediment influx, tectonic subsidence, and global sea-level variations.

Observations of lateral variability and vertical sequences observed in Temblor Formation outcrops are contributing to understanding subsurface geology in Coalinga Field, where the data is widely spaced laterally between points of core control. Erosional surfaces in the outcrop exposures are laterally continuous and easily traced. These surfaces are recognized by their irregular topography and by the presence of bioturbated clay. Based on the characteristics of erosional surfaces in the outcrops, analogous surfaces are identified in cores. Field exposures of incised-valley fills display high relief at the lower contact, pebble lags, and a fining upward trend. Variability in geometry of the lower boundary and stacked fining upward sequences are well defined in the outcrops. Where sharp basal surfaces, pebble lags, and fining upward trends are present in cores, incised-valley fills and their associated geometry are interpreted based on the outcrop analogs. Laterally continuous, well-cemented sand beds containing abundant shell debris are recognized in outcrop exposures as useful marker horizons. Analogous shell beds observed in cores represent laterally extensive zones of low permeability in the subsurface.

In order to develop predictions of flow barriers and subsurface geometries, geological and petrophysical characteristics were compared between outcrops and cores. Using porosity, permeability, and saturation data provided by Chevron, petrophysical data were compared to lithofacies and depositional environments of the Temblor Formation. Analysis included identification of statistical trends for depositional environments and within groups of lithofacies to integrate petrophysical properties with geometries of depositional bodies. Statistical analyses of the Coalinga core data were performed using SPSS (Statistical Package for the Social Sciences) software. Statistical methods include cluster analysis of the fifteen lithofacies present using permeability, porosity, sorting, grain size, and percent sand data. Dendrograms produced from the cluster analysis and frequency-distribution histograms were examined. Lithofacies showing similar statistical characteristics were grouped into five sets.

Geological investigation includes the study of outcrops of the shallow marine Upper Cretaceous Straight Cliffs Formation near Escalante in southern Utah. This area is the site of field permeability testing for the investigation of fractal structure in petrophysical data sets. Lithologic and sedimentologic comparisons between the Coalinga and Escalante sites have been made to facilitate data integration (Table 1). The Escalante research area provides continuous lateral tracing of outcrop exposures, with accessible and well exposed vertical sections. The Coalinga location has a lower degree of well-defined lateral continuity, but shell debris horizons help to provide correlation throughout the field area.

The results from geological field investigation and core study of the Temblor Formation were presented at the annual national meeting of the Geological Society of America (Bridges et al., 1999) and at the annual Pacific Section meeting of the American Association of Petroleum Geologists (Castle et al., 2000). A manuscript on results of the geological investigation of the Temblor Formation is in preparation.

Field Permeability Measurement

A new drill-hole minipermeameter probe (Figure 4) was developed to make measurements of permeability on outcrops at the Escalante field site. This technology has been refined to be a truly reliable field method. Small cylindrical holes are created in an outcrop with a masonry drill, followed by probe insertion, seal expansion and *in situ* calculation of the intrinsic permeability via measurement of the injection pressure, flow rate, and knowledge of the system geometry. Advantages of this approach are elimination of the use of questionable permeability measurements from weathered outcrop surfaces, provision of a superior sealing mechanism around the air injection zone, and its potential for making measurements at multiple depths below the outcrop surface.

The theory for analyzing radial gas flow from a cylindrical hole has been developed. Use of the new probe prescribes a change in the system geometry from that of the more conventional surface probe. It was necessary to derive the mathematical theory for this new type of probe in a way that is analogous to the derivation by Goggin et al. (1988) for the conventional probe. There is a geometric factor for the new probe, which accounts for the system geometry and diverging flow through the domain. In order to determine the geometric factor for the new probe, finite-difference computer simulations were developed to model the pressure-distribution throughout the system. This was begun by verifying the finite-difference solutions of Goggin et al. (1988) for the conventional probe, which applies flow to an exposed rock surface. The work proceeded by modifying the boundary conditions of the simulation to reflect the new drill-hole system geometry, and as a result, the geometric factor for the new system was obtained.

A paper is currently being prepared on the development of the new drill-hole probe for submission to a peer-reviewed journal. A similar presentation at the fall meeting of the American Geophysical Union (Dinwiddie et al., 1999) resulted in information exchange with minipermeameter experimentalists involved in spatial weighting function concepts (Wilson and Aronson, 1999). As a consequence, a paper has been submitted to *Water Resources Research* wherein the physical basis for a spatial weighting function is developed utilizing streamline coordinates (Molz et al., 2000a). Applications of the spatial weighting functions are presented for the conventional surface probe and the new drill-hole probe (Figure 5). Spatial weighting function distributions indicate that with diverging flow-field instruments, such as the gas minipermeameter, porous medium volumes in the inlet vicinity are heavily weighted, with volumes near the seal boundaries shown to be extremely important. The technique described allows one to quantify the size and shape of the sub-volume of a domain contributing to an effective permeability measurement. An abstract has been prepared and submitted to the conveners of the upcoming fall meeting of the American Geophysical Union for a paper elucidating this subject matter (Molz et al., 2000b). Additionally, a comment has been prepared on a recently published paper (Tartakovsky et al., 2000); this comment has been submitted to *Water Resources Research*, and it should clarify some misconceptions and misnomers raised by Tartakovsky and his colleagues by invoking knowledge gained through spatial weighting function concepts (Molz and Dinwiddie, 2000).

Laboratory work with the new drill-hole minipermeameter probe took place during April/May 2000. The following tasks were undertaken: 1) thin section analysis of the rock zone in the immediate vicinity of the drill-hole for the purpose of appraising any damage due to drilling; 2) operator familiarization with achieving

the optimal normal force between the seal and the drill-hole wall; 3) determination of the minimum distance needed between drill-holes to eliminate the possibility of short circuiting gas flow through adjacent holes; and 4) pseudo-calibration of Hassler-sleeve permeability data sets with drill-hole permeability data sets in order to verify order-of-magnitude accuracy. These data sets were obtained from several sandstone boulders, which were transported from the Escalante field site to Clemson University for testing of the new prototype permeability probes. Laboratory testing of the prototype probes in the field-site sandstone facilitated the move to *in situ* measurements near Escalante, Utah. Additionally, the laboratory work indicated general guidelines for field use, such as appropriate pressure and flow rate ranges, expected life of seal material, and the efficacy of obtaining measurements at multiple depths per drill-hole.

The newly designed drill-hole minipermeameter was used during June/July 2000 to obtain data with a sample spacing of 15 cm along horizontal transects and vertical profiles in a portion of the Upper Cretaceous Straight Cliffs Formation at the Escalante field site (Figures 6-12). For each measurement point, grain size and sedimentary structures were observed and recorded. Representative samples were collected for thin-section preparation and petrographic analysis.

The field permeability measurements, which were made at approximately 500 points on a 6 x 21-m sandstone outcrop, demonstrate facies-dependent variations in permeability values and scale. Permeability ranges from 100-800 millidarcies in massive-bedded, poorly to well-sorted, very fine to fine-grained, bioturbated sandstone facies. Permeability in this facies shows relatively little variability (less than plus or minus 25%) over a scale of several meters, which is attributed to homogenization due to burrowing activity. In contrast, permeability ranges from 450 to over 5,500 millidarcies in poor to moderately sorted, fine- to coarse-grained, cross-bedded sandstone facies. Permeability variations and lithologic characteristics in the cross-bedded facies can be correlated between vertical profiles. Both planar-tabular and trough cross-beds, which range from 15-45 cm in thickness, are present in the cross-bedded facies. Permeability in this facies varies by more than an order of magnitude over a scale of only a few cm. This high degree of variability is caused by small-scale variations in grain size and structure related to the depositional processes.

Fractal Analysis

Fractal scaling properties of the data are being analyzed for application in predicting permeability distributions. Analysis of two permeability (k) data sets, collected along two horizontal transects in the bioturbated sandstone facies at the Escalante field site, indicates that horizontal log(k) increment distributions are highly Gaussian (Figure 13, 14). Fractal scaling of log(k) is also observed with a Hurst coefficient of 0.32 (Figure 15), indicating negative correlation of log(k). The plot of log(k) increments versus distance appeared stationary. Results from vertical transects, which included measurements from two different facies, are more variable, but still display Gaussian behavior (Figure 16, 17) to a good approximation with a Hurst coefficient of 0.68 (Figure 18). It is suggested that the fractional Brownian motion (fBm) model may be appropriate for log(k) simulations within a facies.

During the first quarter of 2000, a manuscript (Boufadel et al., in press) on multifractal scaling of intrinsic permeability was accepted for publication in *Water Resources Research.* In this manuscript we were able

to show that data from the Coalinga Oil Field, as well as data obtained in the laboratory using the minipermeameter, displayed multifractal scaling over a significant range of scales.

Conclusion

During the past year, results from field investigations in southern Utah have been compared and integrated with results from study of Temblor exposures in California and from study of cores in Coalinga Field. This type of comparative analysis between Utah and California is yielding a better understanding of the distributions of subsurface geologic and petrophysical properties. Geological observations of lateral variability and vertical sequences observed in outcrops are contributing to prediction of reservoir characteristics in Coalinga Field, where geologic and petrophysical data are limited to points of well control. Analysis of permeability data from Coalinga Field has lead to identification of statistical trends for depositional environments and for groups of lithofacies.

A new minipermeameter probe was developed for measurement of outcrop permeability. This new probe was designed and built to perform *in situ* permeability measurements in small-diameter drill holes. Advantages of this method are:

1) measurement of permeability below the weathered zone of outcrop surfaces;
2) a superior sealing mechanism around the air injection zone; and
3) potential for making measurements at multiple depths below the outcrop surface.

Use of the new drill-hole minipermeameter probe in southern Utah during summer 2000 provided data needed for fractal analysis. Quality of the data and durability of the instrument confirm that that the new technology is a robust and viable field method.

Using the new drillhole probe, outcrop permeability measurements from the shallow-marine Upper Cretaceous Straight Cliffs Formation near Escalante, Utah, demonstrate facies-dependent variations in permeability values and scale. Permeability ranges from 100-800 millidarcies in massive-bedded, poorly to well-sorted, very fine to fine-grained, bioturbated sandstone facies, showing relatively little variability (<+/-25%) over a scale of several meters, which is attributed to homogenization due to burrowing. In contrast, permeability ranges from 450-5,500 millidarcies in poor to moderately sorted, fine- to coarse-grained, cross-bedded sandstone facies. Permeability in this facies varies by more than an order of magnitude over a scale of only a few cm. The contrast in permeability variation between the bioturbated facies and the cross-bedded facies has important implications for subsurface fluid-flow prediction using outcrop analogs.

Analysis of permeability (k) data sets collected along horizontal transects in the bioturbated sandstone facies indicates that horizontal log(k) increment distributions are highly Gaussian. Fractal scaling of log(k) is also observed with a Hurst coefficient of 0.32, indicating negative correlation of log(k). Results from vertical transects, which include measurements from both the bioturbated sandstone facies and the cross-bedded sandstone facies, are more variable, but still display Gaussian behavior to a good approximation with a Hurst coefficient of 0.68.

Results from geological investigation, permeability testing, and fractal analysis are being integrated to produce conditioned, three-dimensional computer models for reservoir characterization of Coalinga Field.

References

Boufadel, M.C., S. Lu, F.J. Molz and D. Lavallee. Multifractal scaling of intrinsic permeability. *Water Resources Research*, in press.

Bridges, R. A., J. W. Castle and M. S. Clark. Depositional patterns and sequence stratigraphy of the Miocene Temblor Formation, San Joaquin Basin, California. *Geological Society of America Abstracts with Programs*, v. 31, no. 7, p. A-425. Denver, CO, October 1999.

Castle, J.W., R.A. Bridges, C.L. Dinwiddie, F.J. Molz, and M.S. Clark. Comparisons between cores and surface exposures of the Miocene Temblor Formation, Coalinga Field, San Joaquin Basin: Applications to reservoir characterization. *American Association of Petroleum Geologists Pacific Section Meeting Program and Abstracts*, p. A8. Long Beach, CA, June 2000.

Dinwiddie, C.L., F.J. Molz, III, L.C. Murdoch and J.W. Castle. A new mini-permeameter probe and associated analytical techniques for measuring the *in situ* spatial distribution of permeability. *American Geophysical Union, EOS*, v. 80, no. 46. San Francisco, CA, December 13-17, 1999.

Goggin, D.J., R.L. Thrasher and L.W. Lake. Experimental analysis of minipermeameter response including gas slippage and high velocity flow effects. University of Texas at Austin, July 1988.

Molz, F.J., and C.L. Dinwiddie. Comment on "Kinematic structure of mini-permeameter flow" by Daniel M. Tartakovsky, J. David Moulton and Vitaly A. Zlotnik. *Water Resour. Res*. In review, 2000.

Molz, F.J., C.L. Dinwiddie and J.L. Wilson[a]. What does an instrument measure? A physical basis for calculating spatial weighting functions applicable to hydraulic conductivity and intrinsic permeability measurements. *Water Resour. Res*. In review, 2000.

Molz, F.J., C.L. Dinwiddie and J.L. Wilson[b]. Development of a physical basis for calculating spatial weighting functions, with application to the gas mini-permeameter. *American Geophysical Union, EOS*, v. 81, no. 46. San Francisco, CA, December 15-19, 2000

Tartakovsky, D.M., J.D. Moulton and V.A. Zlotnik. Kinematic structure of minipermeameter flow, *Water Resour. Res.*, v. 36, p. 2433-2422, 2000.

Wilson, J.L., and E.C. Aronson. Calculating instrument spatial filter functions: Illustration for the gas minipermeameter. *American Geophysical Union, EOS*, v. 80, no. 46. San Francisco, CA, December 13-17, 1999.

Escalante, Utah	Coalinga, California
Straight Cliffs Formation	Temblor Formation
Late Cretaceous (Turonian)	Early to Middle Miocene (Saucesian, Relizian, Luisian)
Lithology: cross-bedded medium-grained sandstone; bioturbated fine-grained sandstone; interlaminated to interbedded shale and very fine to fine-grained sandstone; shell and pebble lags; mud rip-up clasts	Lithology: cross-bedded fine- to medium-grained sand; bioturbated coarse-grained sand; interlaminated to interbedded clay and fine-grained sand; fossiliferous sand; diatomaceous silt and clay; quartz and lithic pebble lags; mud rip-up clasts
Sedimentary Structures: trough and planar-tabular cross-bedding; horizontal lamination; ripple cross-lamination	Sedimentary Structures: trough and planar-tabular cross-bedding; clay drapes on foresets; ripple cross-lamination; bi-directional cross-bedding; mottled bedding
Biological Features: ¼" to ½" diameter vertical and horizontal burrows, filled with sand; wood and plant fragments	Biological Features: ¼" to 1" diameter vertical and horizontal burrows, clay lined and some sand filled; meniscus burrows present on some erosional surfaces; wood fragments
Depositional Environments: Estuarine, with fluvial incised valley-fill below; tidal shoreline above	Depositional Environments: Incised valley-fill, estuarine, tide- and wave dominated shoreline, regressive tidal and coastal plain

Table 1. Geologic comparison of Escalante site with Coalinga site.

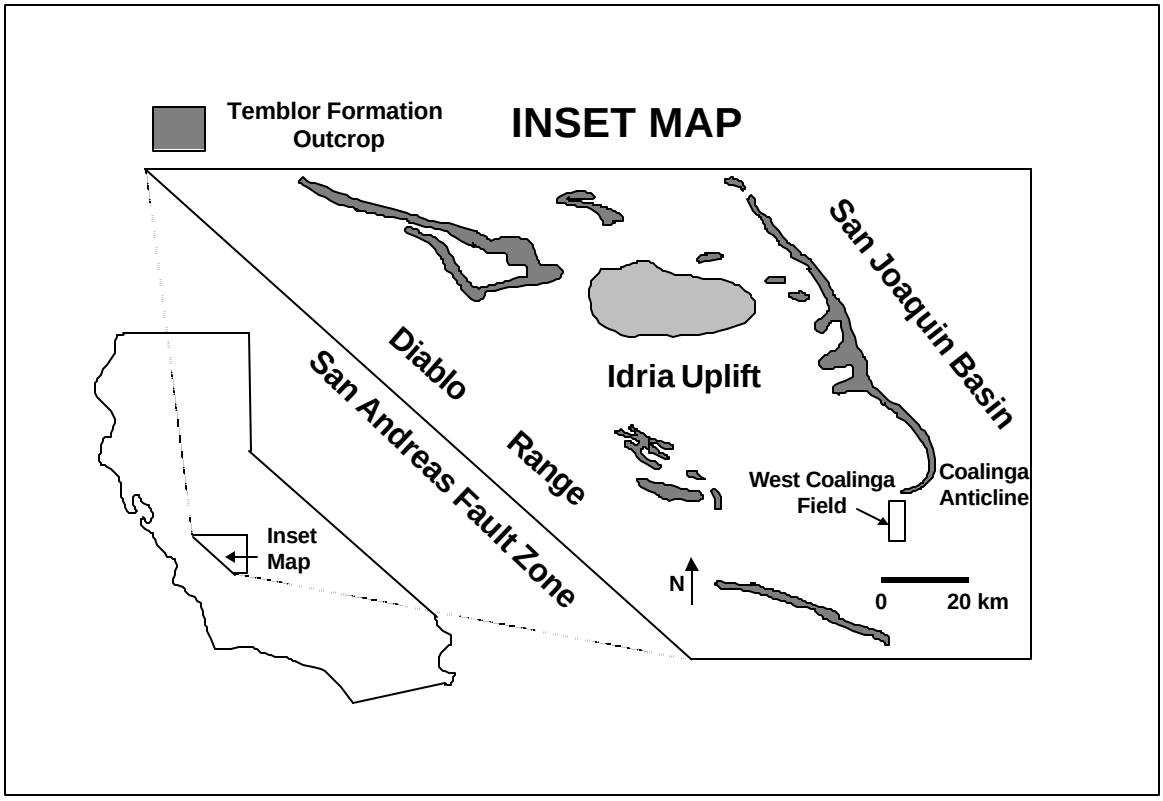

Figure 1. Location map of the Coalinga area, California

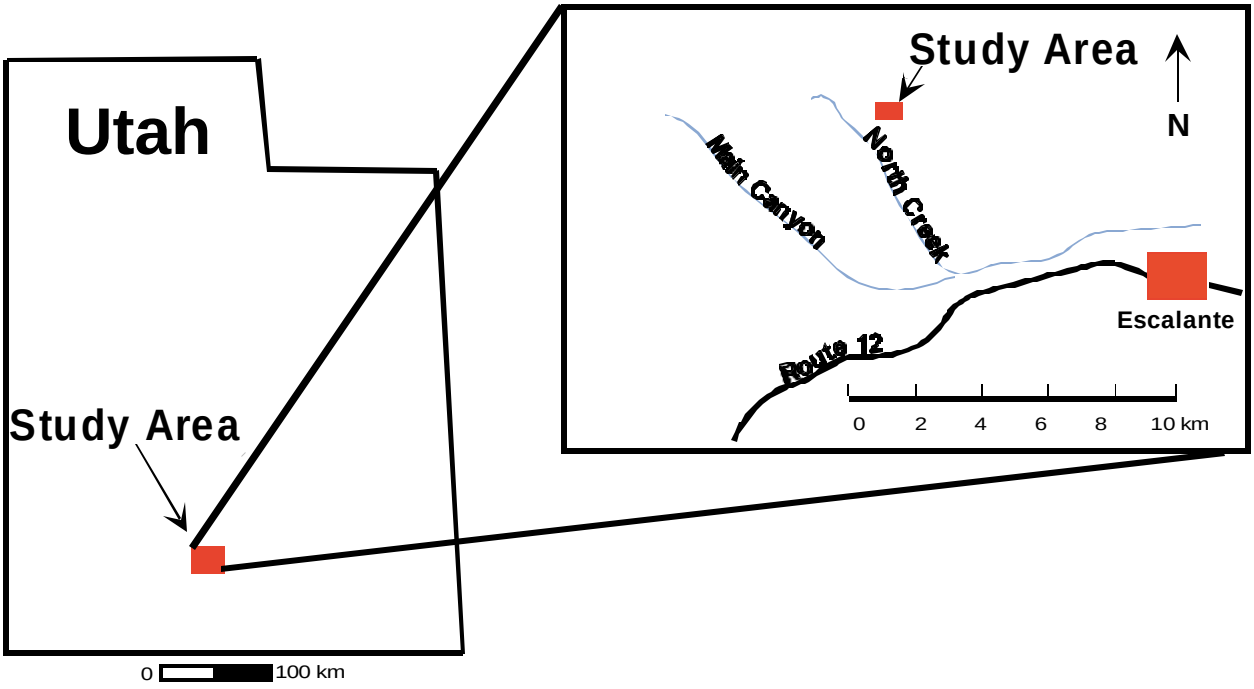

Figure 2. Location Map for field site near Escalante, Utah.

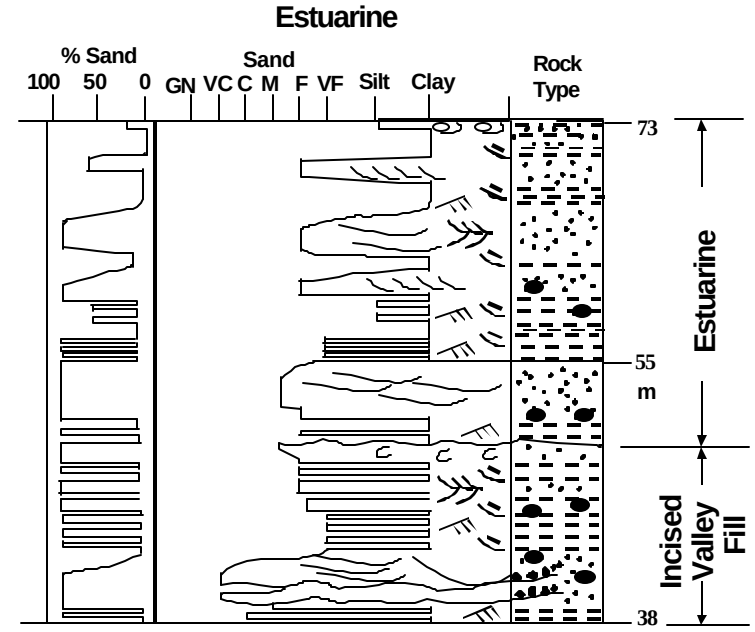

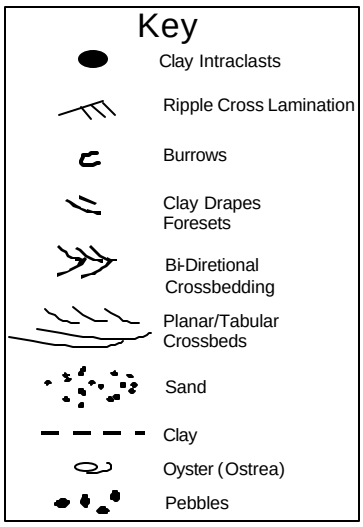

Figure 3. Outcrop description from Laval Grade, Coalinga area, California, showing incised valley fill and estuarine deposits. From Bridges et al. (1999).

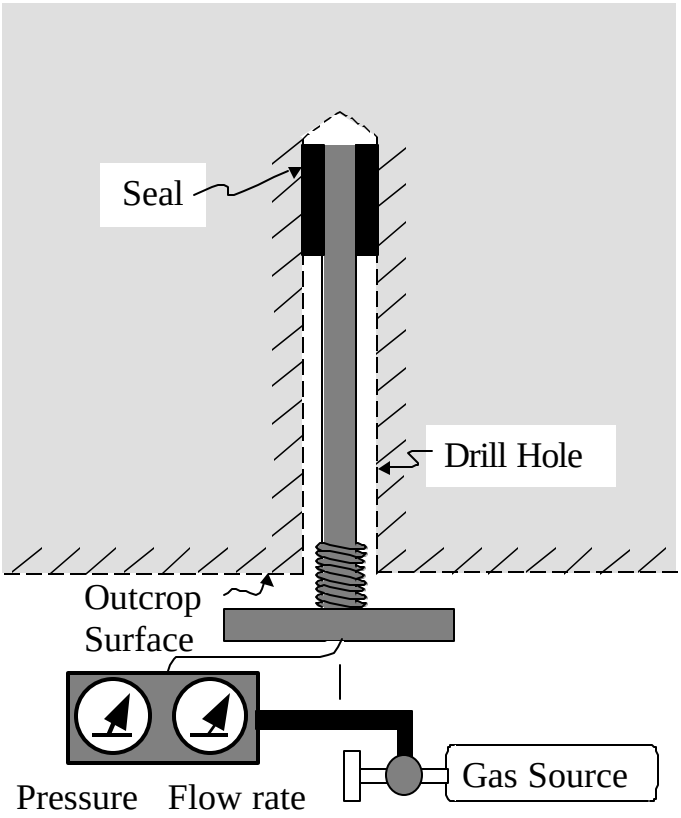

Figure 4. Schematic of the new drill-hole mini-permeameter designed for steady-state *in situ* field measurements.

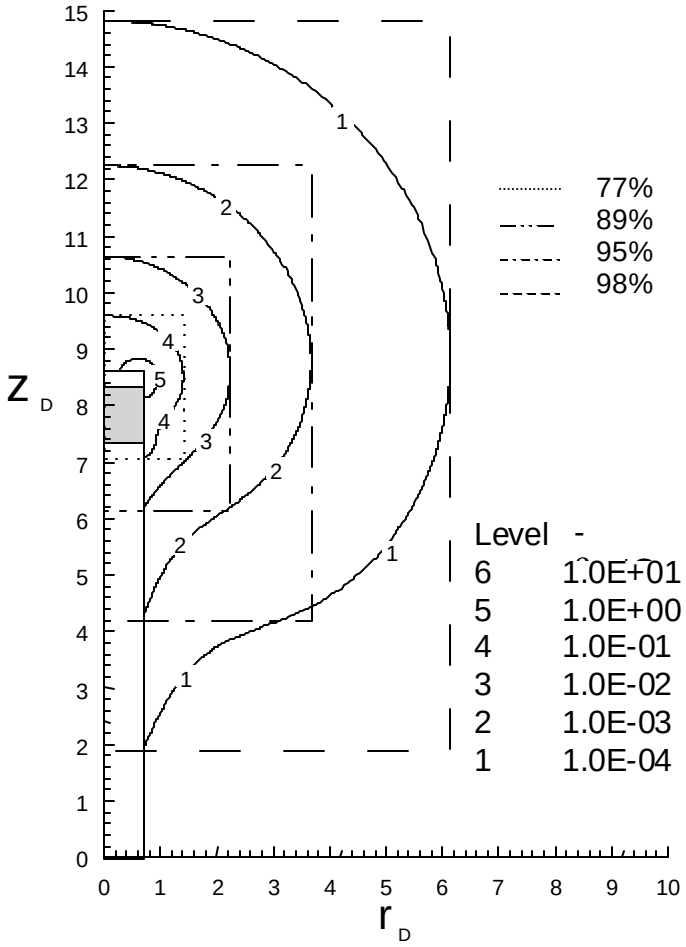

Figure 5. Lines of equal pseudo-potential gradient squared, which are proportional to the dimensionless spatial weighting function, are displayed as curvilinear contours. When integrated, the spatial weighting function over the entire flow domain must sum to 1. By numerically integrating the spatial weighting function over smaller volumes in the vicinity of the inlet, the averaging volume of the instrument becomes apparent. This is illustrated by the concentric cylinders, indicated by variously dashed lines, which increasingly encompass greater percentages of the spatial weighting function.

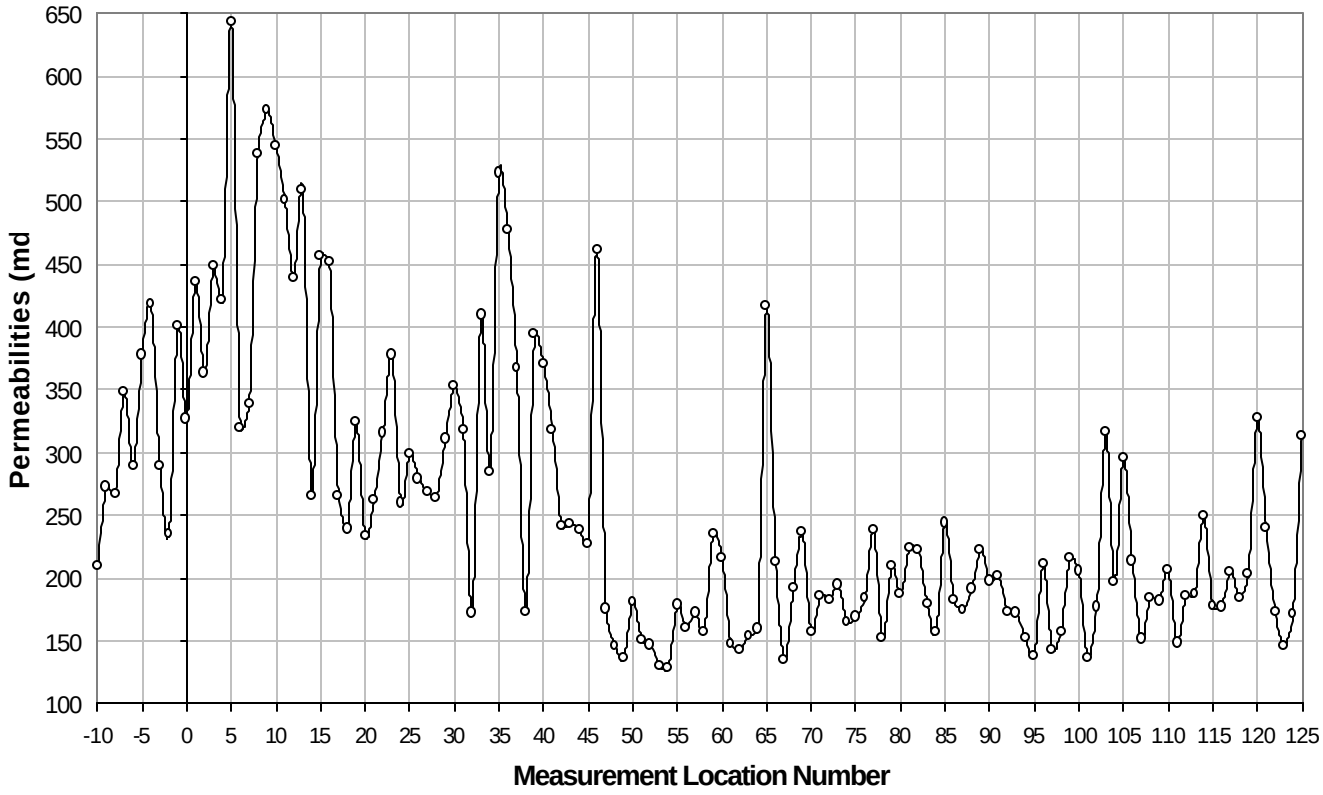

Figure 6. Permeability distribution along transect D: the lowermost transect studied in the bioturbated facies. Measurements were made at 15 cm intervals.

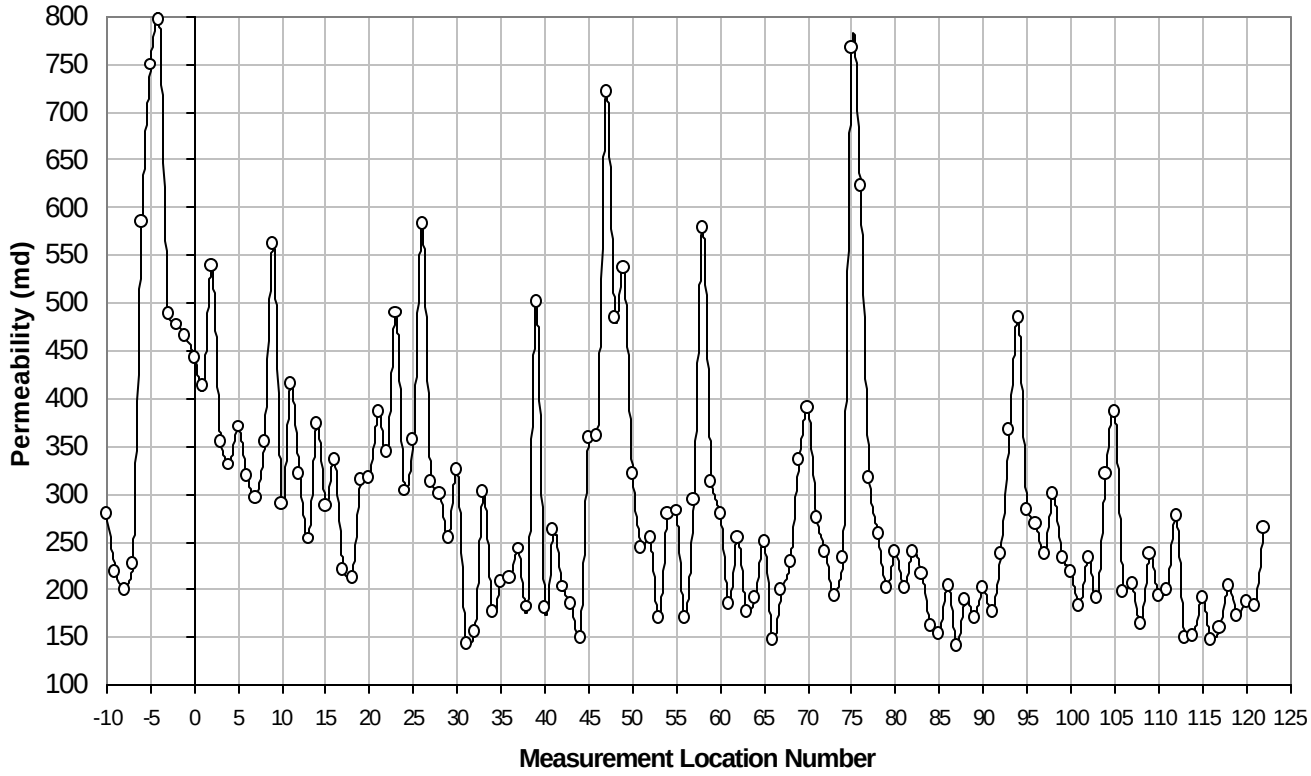

Figure 7. Permeability distribution along transect H: the uppermost transect studied in the bioturbated facies. Measurements were made at 15 cm intervals.

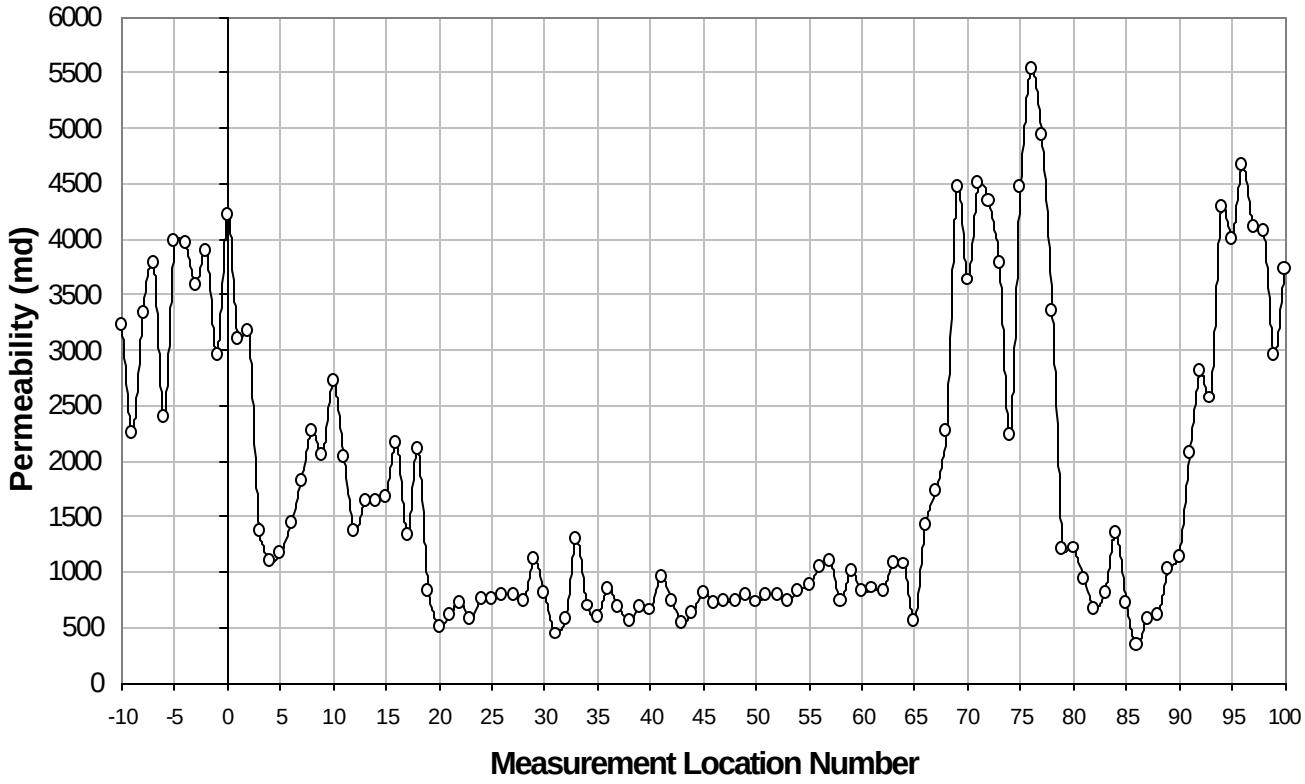

Figure 8. Permeability distribution along transect X: the transect studied in the cross-bedded facies. Measurements were made at 15 cm intervals.

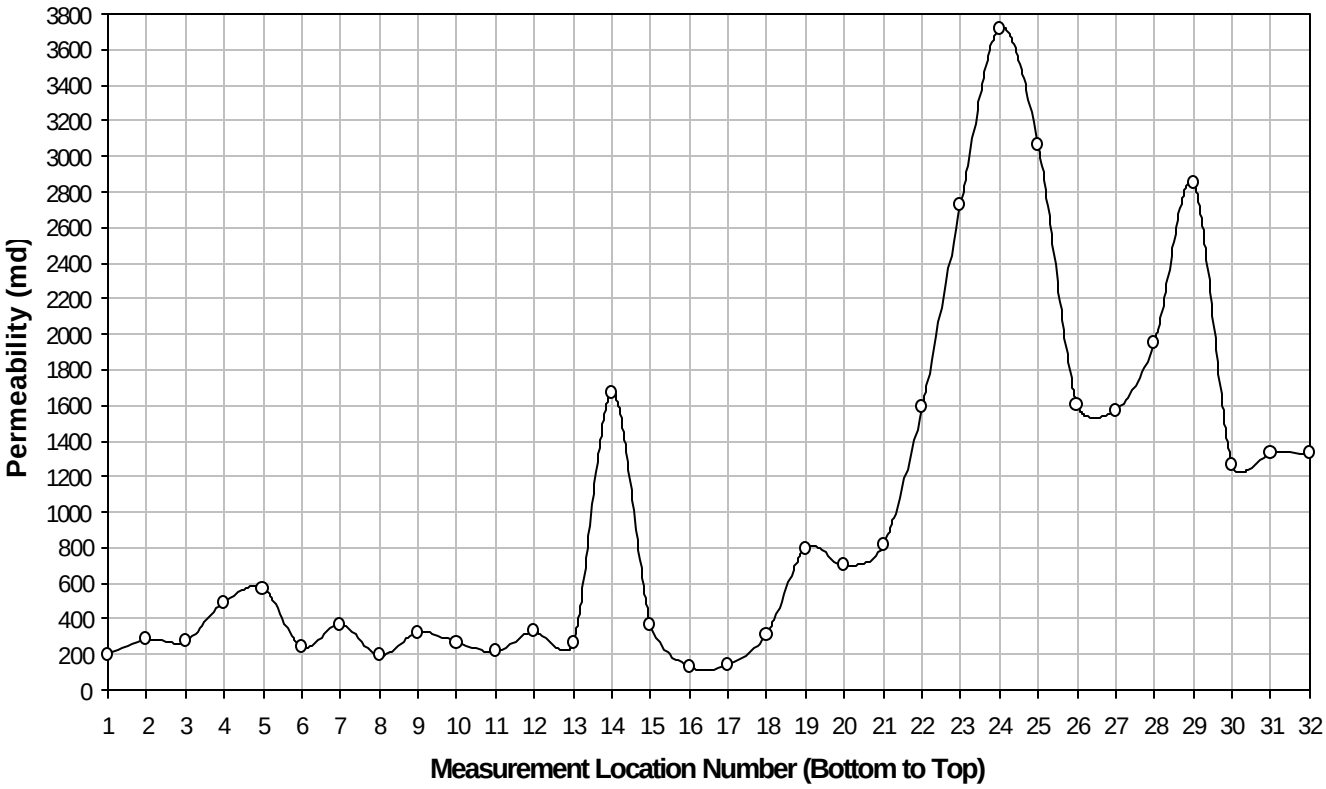

Figure 9. Permeability distribution along transect V1: the first vertical transect (from left to right) studied. Measurements were made at 15 cm intervals.

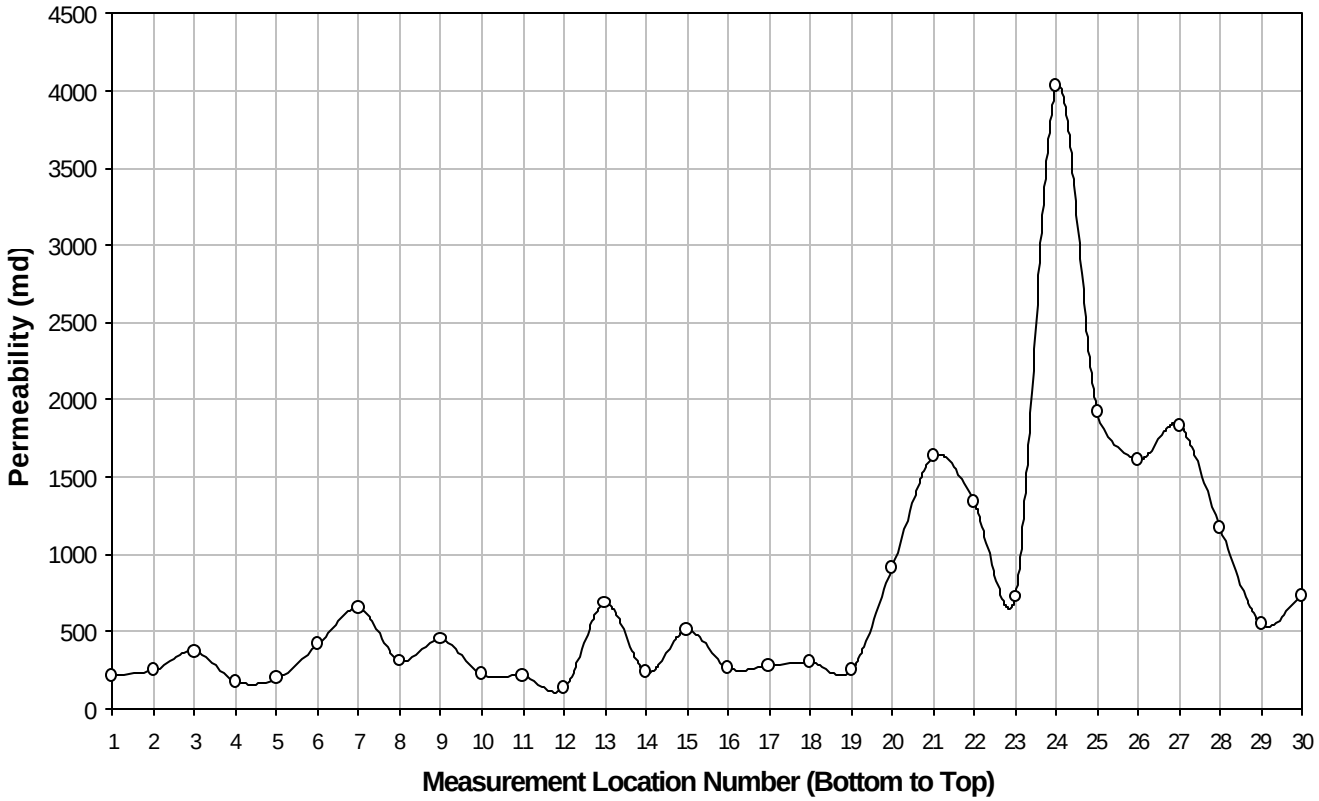

Figure 10. Permeability distribution along transect V2: the second vertical transect (from left to right) studied. Measurements were made at 15 cm intervals.

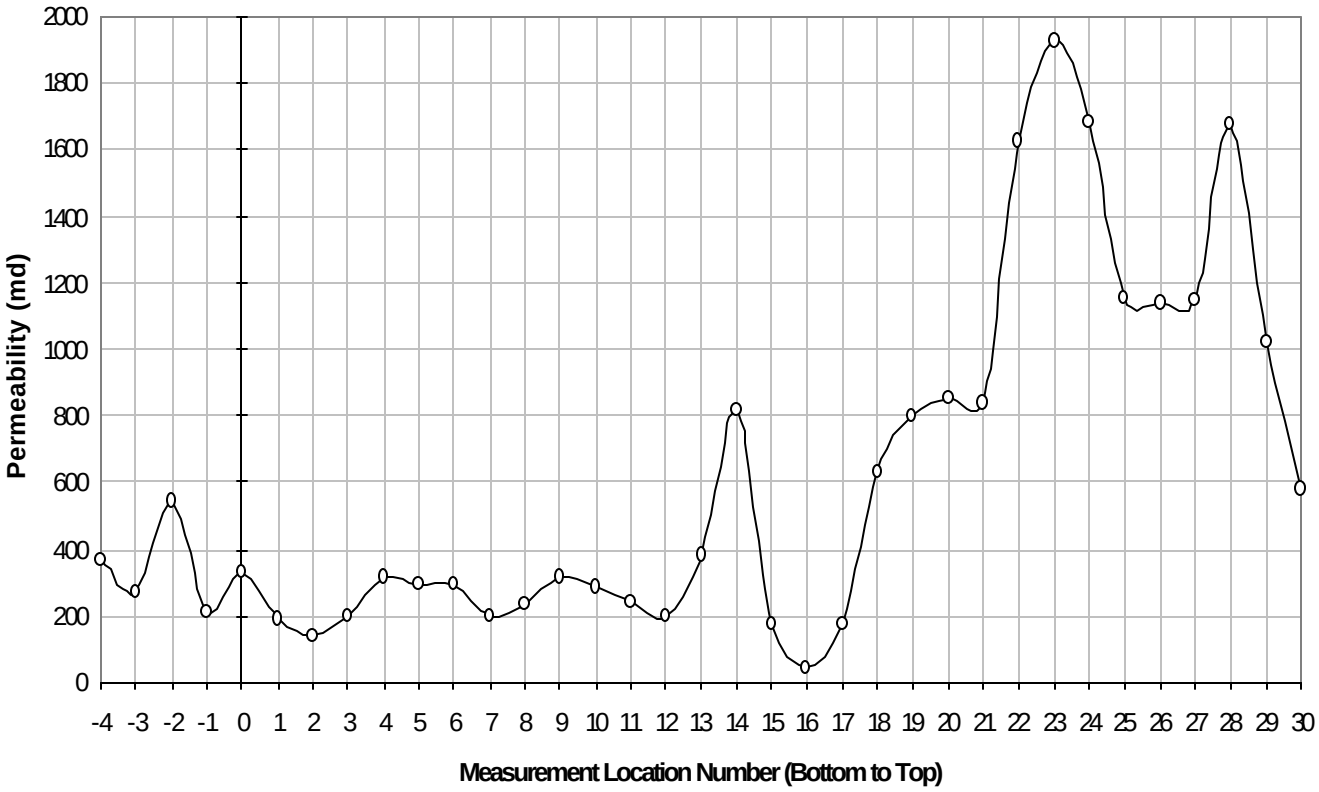

Figure 11. Permeability distribution along transect V3: the third vertical transect (from left to right) studied. Measurements were made at 15 cm intervals.

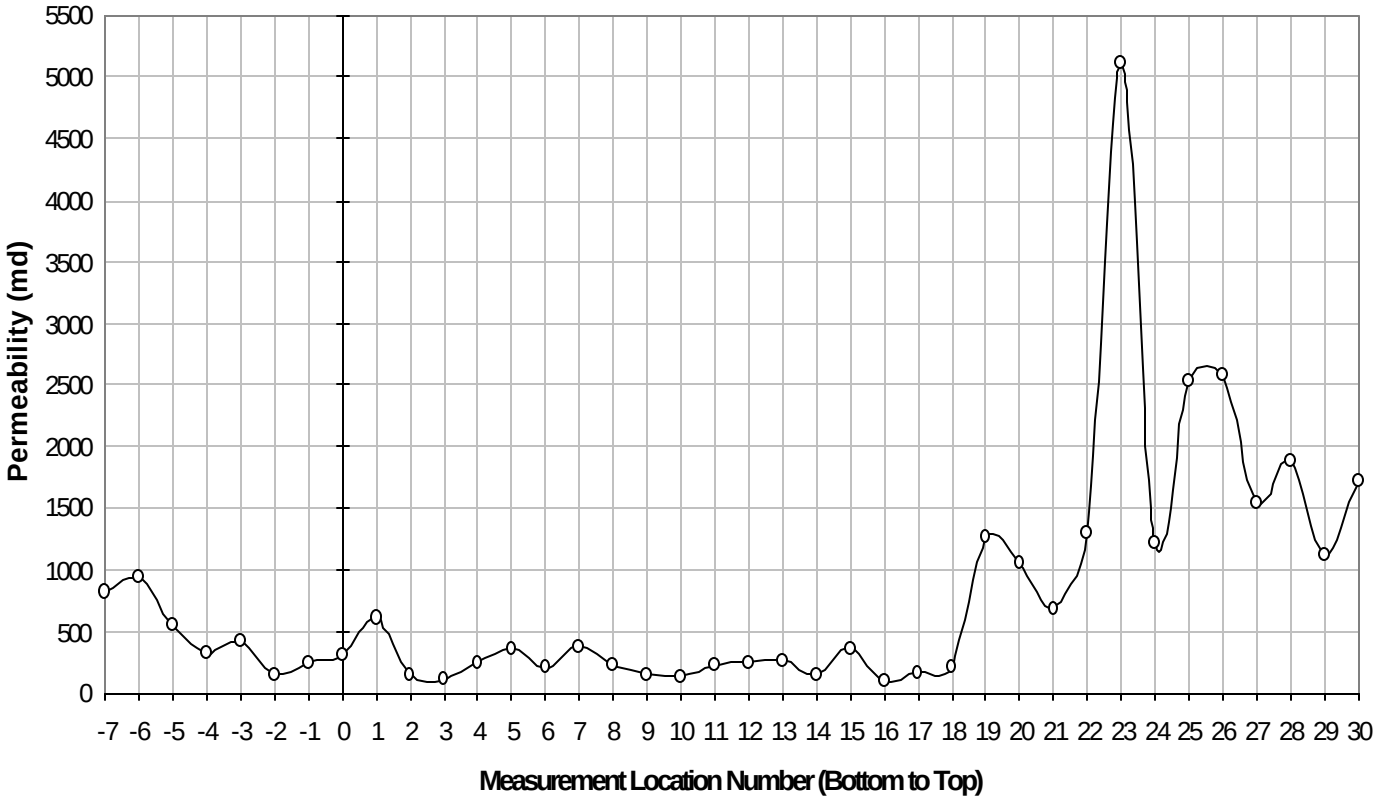

Figure 12. Permeability distribution along transect V4: the fourth vertical transect (from left to right) studied. Measurements were made at 15 cm intervals.

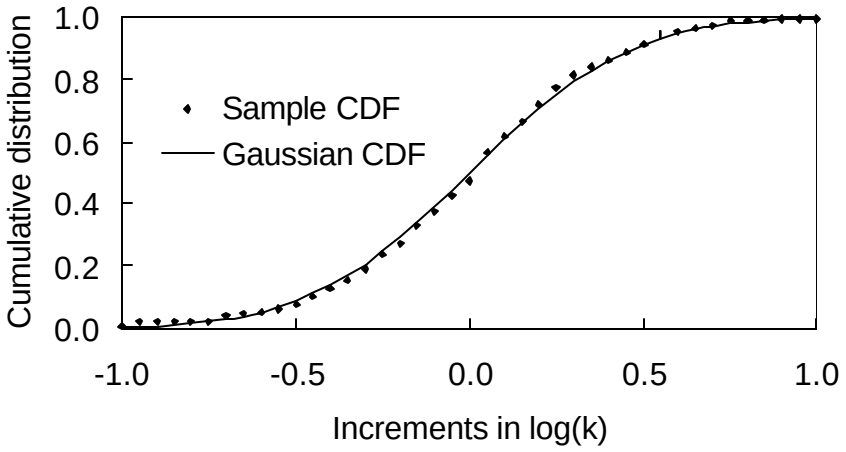

Figure 13. Probability distribution of log(k) increments in the horizontal direction

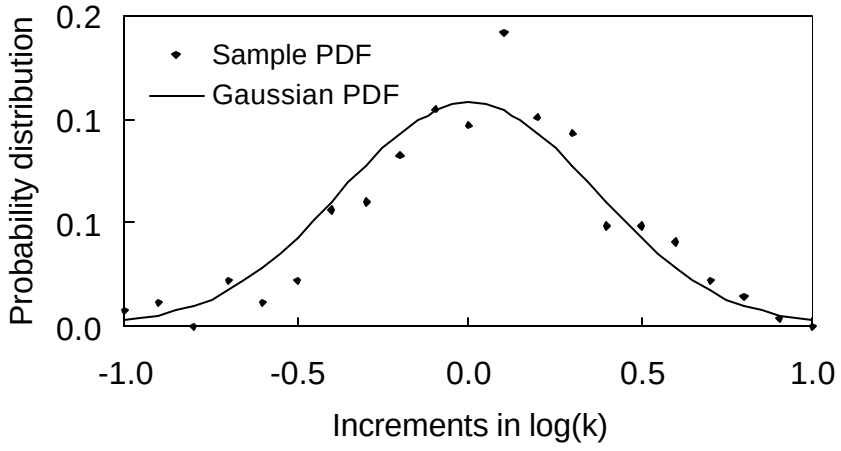

Figure 14. Cumulative distribution of log(k) increments in the horizontal direction

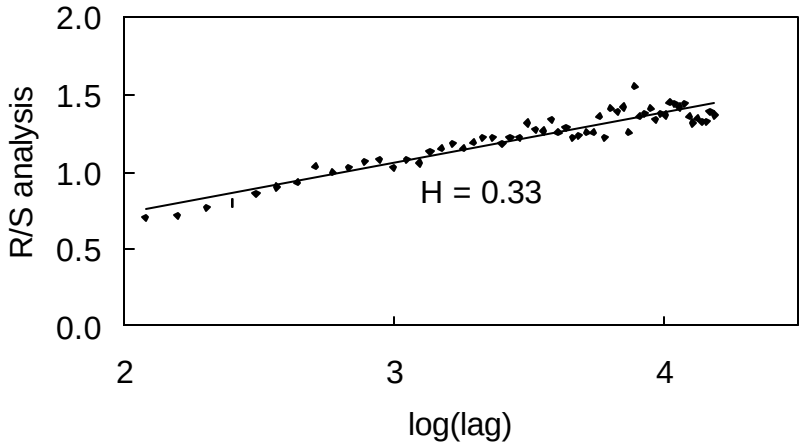

Figure 15. Rescaled range analysis of log(k) in the horizontal direction

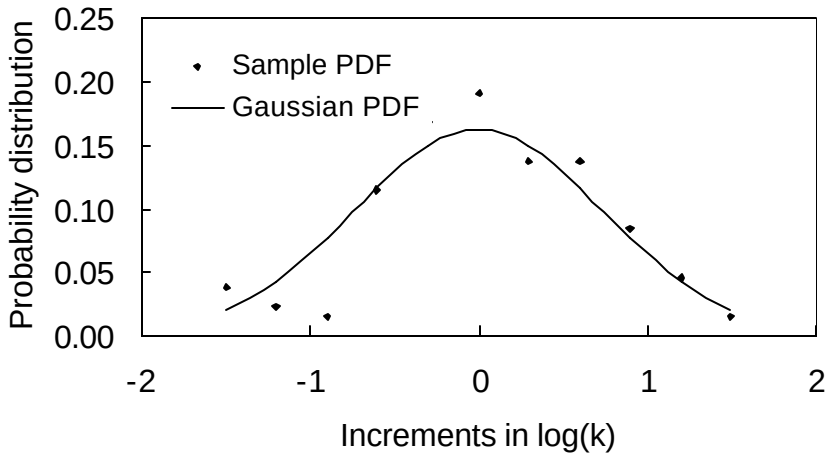

Figure 16. Probability distribution of log(k) increments in the vertical direction

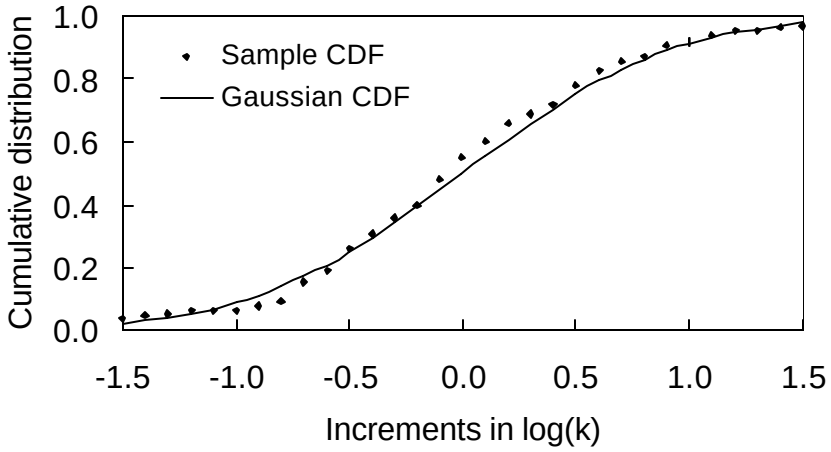

Figure 17. Cumulative distribution of log(k) increments in the vertical direction

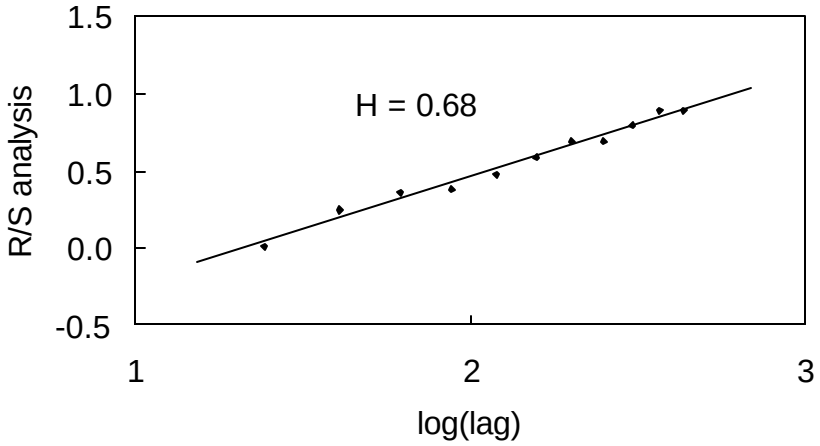

Figure 18. Rescaled range analysis of log(k) in the vertical direction